Analysis of the effect of rear-window tilt on aerodynamic drags of sedan vehicle model

Conference Paper · April 2023

DOI: 10.1063/5.0126980

CITATIONS
0

READS
34

4 authors:

Nasaruddin Salam
Universitas Hasanuddin
31 PUBLICATIONS **139** CITATIONS
SEE PROFILE

Rustan Tarakka
Universitas Hasanuddin
39 PUBLICATIONS **119** CITATIONS
SEE PROFILE

Rudiansyah ..
Universitas Hasanuddin
1 PUBLICATION **0** CITATIONS
SEE PROFILE

Muhammad Ihsan Mukrim
LLDIKTI IX Sulawesi
50 PUBLICATIONS **83** CITATIONS
SEE PROFILE

RESEARCH ARTICLE | APRIL 25 2023

Analysis of the effect of rear-window tilt on aerodynamic drags of sedan vehicle model

Nasaruddin Salam; Rustan Tarakka ✉; Rudiansyah; ... et. al

AIP Conference Proceedings 2630, 020027 (2023)
https://doi.org/10.1063/5.0126980

Analysis of the Effect of Rear-Window Tilt on Aerodynamic Drags of Sedan Vehicle Model

Nasaruddin Salam[1, a)], Rustan Tarakka[1, b)] , Rudiansyah[1, c)] , Muhammad Ihsan Mukrim[2, d)]

[1]*Department of Mechanical Engineering, Hasanuddin University, Gowa., Indonesia*
[2]*Sekolah Tinggi Teknik Baramuli, Pinrang. Indonesia*

[a)] nassalam.unhas@yahoo.co.id
[b)] Corresponding author: rustan_tarakka@yahoo.com
[c)] ransyah205@gmail.com
[d)] muhammadihsan@alumni.ait.asia

Abstract. Aerodynamic drag is influenced by the geometry of the front, windshield, roof, and rear of the vehicle. Most of the drag on the vehicle is due to the low pressure and flow separation at the rear of the vehicle. Therefore, one of the efforts that can be made to reduce aerodynamic drag is changing the shape of the vehicle model, especially at the rear window tilt angle. This study aims to analyze the effect of changing the shape of the rear window on the aerodynamic drag of the sedan vehicle model. The object of this research is a sedan vehicle model with a front window tilt of 25º. The research was carried out using two approaches, namely a computational approach using a computational fluid dynamics program and an experimental approach using a subsonic wind tunnel. The rear window tilt angle of the sedan model is set at an angle of 20º, 23º, 25º, 27º, and 30º, and the upstream speed was set at 19.4 m/s. The results showed that the change in the shape of the rear window has an effect on the flow separation and turbulence developed at the rear of the sedan vehicle model. It also affects the pressure coefficient and aerodynamic drag. The smallest aerodynamic drag coefficient is obtained at the rear-window tilt angle of 20º, gaining 0.691 for the computational approach, and 0.665 for the experimental approach.

INTRODUCTION

One of the references to the development of automobile is in the design of shape of the vehicle's body. The development is aimed to gain more aerodynamic body shapes to deminish the drag. Overtime, the design of car shapes is everchanging, not only to adapt with modern trends, but also in engineering point of views, including the aerodynamic drag [1] [2] [3].

In general, a moving car will experience aerodynamic drags caused by fluid flow that comes into direct contact with the car body. Large aerodynamic drags are caused by a decrease in pressure and flow separation that occurs in the rear of the car [4] [5]. Flow separation that occurs at the velocity boundary layer of fluid flow and solid surface of the car will form a backflow [6] [7]**.**

For objects moving in a viscous fluid, the drag forces and the lift forces are strongly related the to flow separation [8]**.** The separation of the flow will cause a wake behind the cylinder that results in drag. The earlier the emergence of the flow separation, the wider the wake so that the greater the drag aerodynamic drag contribution in the vehicle is influenced by the geometry of the car's front, windshield, roof and rear that have been determined by various models through testing and numerical calculations [9] . In recent days, aerodynamic drag in cars can be known easily through experimental and computational processes.

Various types of passenger cars circulate in the market, in terms of design, manufacturer, and engine capacity. The common car accommodates 5-7 people and has an engine with large power that is adjusted to its carrying ability with a body shape that does not consider aerodynamic aspects so that the drag force experienced is considerably large.

Proceeding of International Conference on Energy, Manufacture, Advanced Material and Mechatronics 2021
AIP Conf. Proc. 2630, 020027-1–020027-11; https://doi.org/10.1063/5.0126980
Published by AIP Publishing. 978-0-7354-4453-9/$30.00

Most of the drag forces appear on the car due to low pressure and separation of flow at the back of the car. The earlier the emergence of the flow separation, the greater the wake formation behind the vehicle.

In the fluid dynamics review, methods to reduce aerodynamic drag can be achieved by modifying the flow of air through the vehicle body and delaying separation and reducing the development of the recirculation area at the back of theseparated swirling structure [10]

The computational approach using fluent CFD 6.3 software was used in this study with the aim of investigating the effect of the placement of fin and suction on the aerodynamic constraints of vehicle models.

RESEARCH METHODOLOGY

The object of the research used is the body of a sedan model car. As a reference material, dimensions are used in experiments with a scale of 1: 32. The 1:32 scale to the original model was used to facilitate the experiment, and reduced the cost for the manufacture of the model in Figure 3.1. with dimensions of length 138.28 mm, width 54.06 mm, height 40.63 mm, front angle 25° and rear angle 25°. This research was conducted by changing the shape of the rear window tilt angle of the test model. Where there are four treatments of test models, namely rear rear window tilt of 20°, 23°, 27°, and 30°. The test model with a 25° rear angle is seen in figure 1.

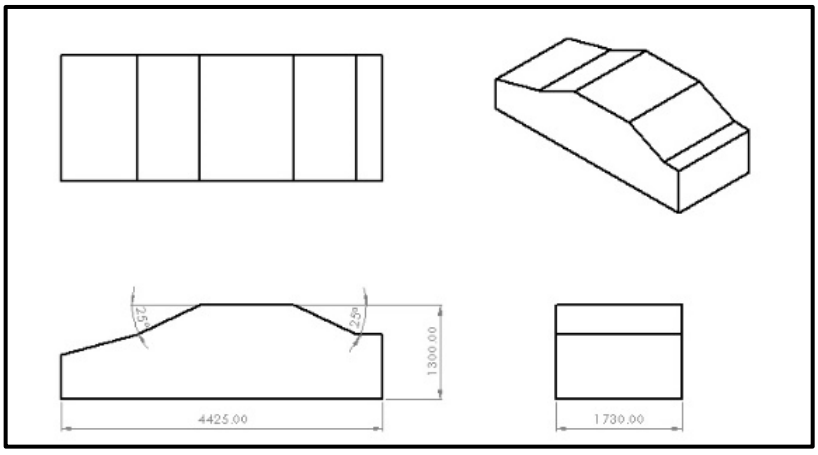

FIGURE 1. Rear angle test model dimensions 25º

In this study, a computational approach was used using the CFD Fluent 6.3 software with a standard k-epsilon turbulence model with equations as shown in the Eq. 1 and the Eq. 2.

a. Kinetic Energy

$$\frac{\partial}{\partial t}(\rho k) + \frac{\partial}{\partial x_i}(\rho k u_i) = \frac{\partial}{\partial x_j}\left[\left(\mu + \frac{\mu_t}{\sigma_k}\right)\frac{\partial k}{\partial x_j}\right] + P_k + P_b - \rho_\epsilon - Y_M + S_k \quad (1)$$

b. Dissipation Rate

$$\frac{\partial}{\partial t}(\rho\in) + \frac{\partial}{\partial x_i}(\rho\in u_i) = \left[\left(\mu + \frac{\mu_t}{\sigma_\epsilon}\right)\frac{\partial \epsilon}{\partial x_j}\right] + C_{1\epsilon}\frac{\epsilon}{k}(P_k + C_{3\epsilon}P_b) - C_{2\epsilon}\rho\frac{\epsilon^2}{k} + S_\epsilon \quad (2)$$

The relationship of drag force and the drag coefficient that occurs on the vehicle model is displayed in Eq. 3.

$$C_D = \frac{F}{\frac{1}{2}\rho U^2 A} \quad (3)$$

The type of meshing used is tet/hydrid type hex core. with the boundary conditions seen in Table 1.

TABLE 1. Computing boundary conditions

Boundary Conditions	Type	Value
Inlet	Velocity Inlet	19.4 m/s
Outlet	Pressure Outlet	-
Model	Wall	-
Wall/Wind Tunnel	Wall	-

The computational approach includes data retrieval pressure distribution, intended to support the aerodynamic drag results of the vehicle model. Basically, for the applications on vehicle model, aerodynamic drag reduction is characterized by an increase in pressure field on the rear wall of the vehicle model. The location of the data collection can be seen in the area behind the object in 8 points (15, 16, 17, 20, 21, 22, 23 and 24). It is also focused on how many different areas, at the top of the 16 points (5, 6, 7, 8, 9.1 0, 11, 12, 13, 14, 15, 16, 17, 18 and 19) and the front of the 11-point test model (1, 2, 3, 4, 5, 6, 7.8 9, 10 and 11), resulting in data of 24 points for the models presenting pressure coefficients. Details of the location of the pressure distribution data capture are displayed in Figure 2.

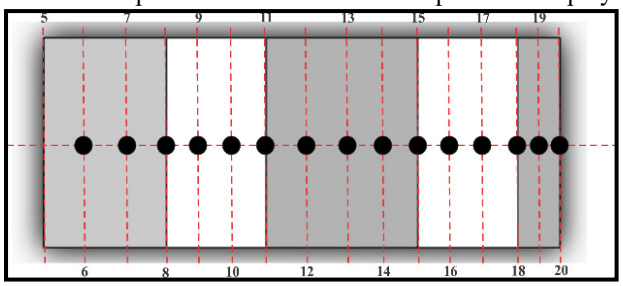

(a) Top view

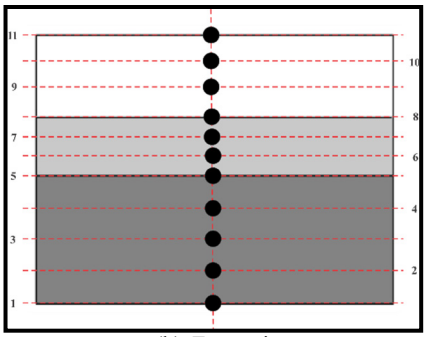

(b) Front view

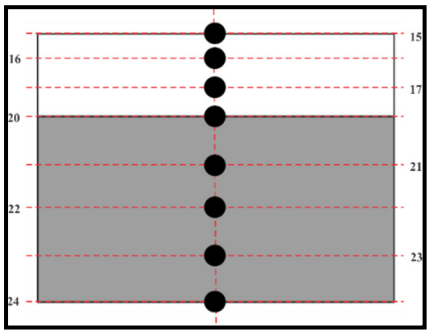

(c) Rear view

FIGURE 2. Location of pressure field data retrieval on the test model

RESULTS AND DISCUSSIONS

Flow characteristics

The flow characteristics of the rear window of test model with an initial tilt angle of 25˚, and subsequently varied at 20˚, 30˚, 27˚, and 30˚, using the upstream velocity shown in figure 3.

In figure 3 part a shows the flow separation that occurs in the rear angle test model 25. The separation of the flow is caused by the flowing fluid can no longer follow the surface shape of the test model. The separation of streams results in a backflow on the back of each test model that forms a olakan. The backflow arises due to the appearance of negative pressure that causes the phenomenon of suction towards the back. Suction towards the back is the main cause of the magnitude of drag on the test model. In addition to flow separation, the drag is also caused by the appearance of a vortex on the back of the test model. This is due to the difference in speed in the area close to the rear window angle of the model .

In figure 3 parts b and c show the vortex formed experiencing a slight decrease where the shape of the vortex is somewhat thin when compared to the angle of 25˚.This indicates that the effect of changes in shape on the rear window can affect. Because for the shape of the flow that passes through the surface through the separation delay. So that the wake and vortex that formed are somewhat reduced. The best separation delay is at the rear window tilt of 20°. Where the shape resembles a fastback car that can minimize the wake area itself.

In figure 3 parts d and e show the wake and vortex getting bigger when compared to 25° tilt angle. This happens because the shape of the model undergoes earlier separation on its surface.

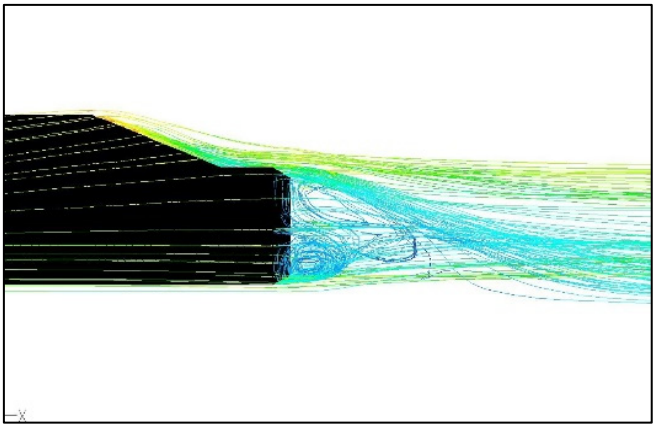

(a) Rear window tilt 25º

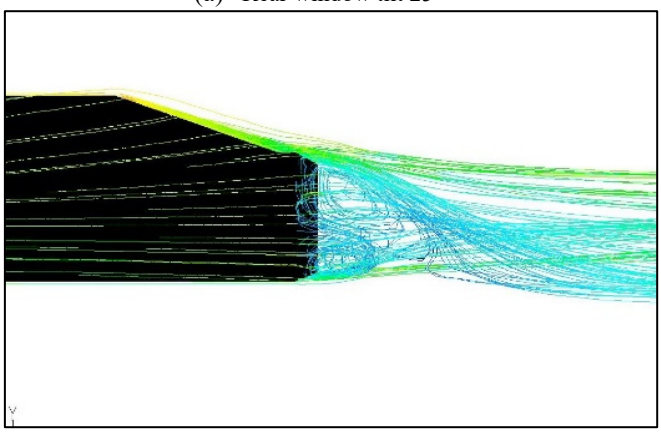

(b) Rear window tilt 20º

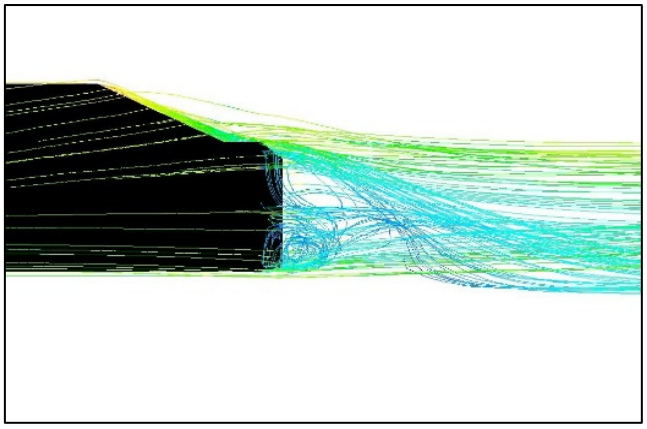

(c) Rear window tilt 23º

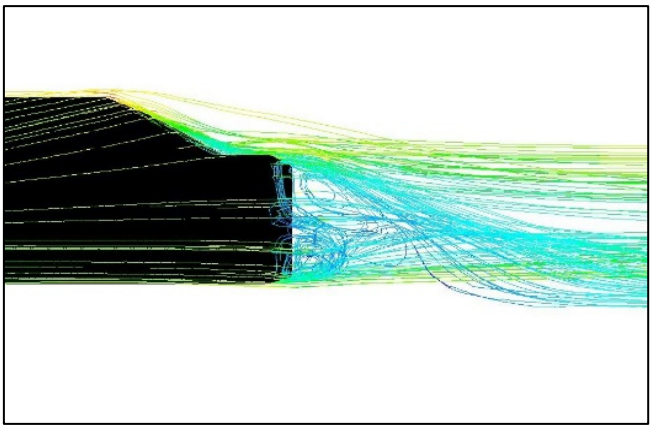

(d) Rear window tilt 27º

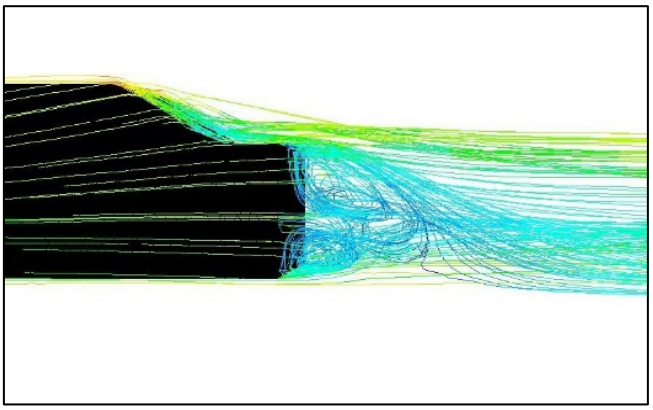

(e) Rear window tilt 30º

FIGURE 3. Pathline speed with rear window tilt angle variations (a) Rear window tilt 25º (b) Rear window tilt 20º (c) Rear window tilt 23º (d) Rear window tilt 27º (a) Rear window tilt 30º

Pressure coefficient

The pressure coefficient values on the test model with changes in rear window tilt shape variation by looking at the location of the data capture in figure 2. The negative pressure coefficient value in the back area of the test model indicates the presence of a suction phenomenon towards the back that causes drags in the test model. The pressure coefficient value of the computing result with an upstream speed of 19.4 m/s is displayed in graphs. The pressure distribution on vehicle model with the rear window tilts of 20° and 25° is seen in figures 4 and 5. From the graph it can be seen that at the rear window tilt of 20° has a larger distribution when compared to the tilt angle of 25°. This happens because the change in the rear window tilt of 20° is experiencing separation delays so that the pressure value of the suction area increases.

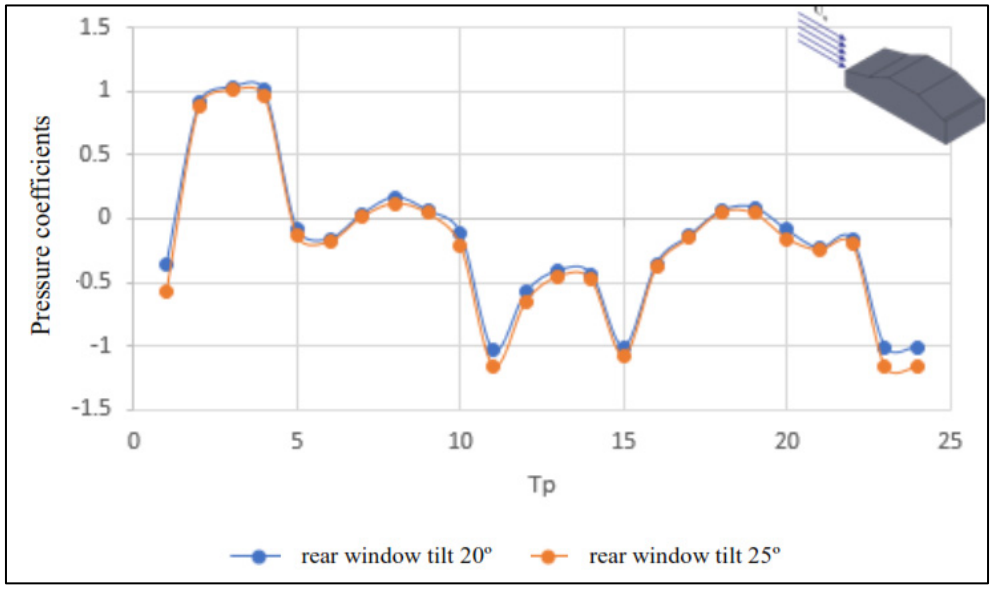

FIGURE 4. Comparison of pressure distribution on 20° and 25° rear window tilts for computational approach

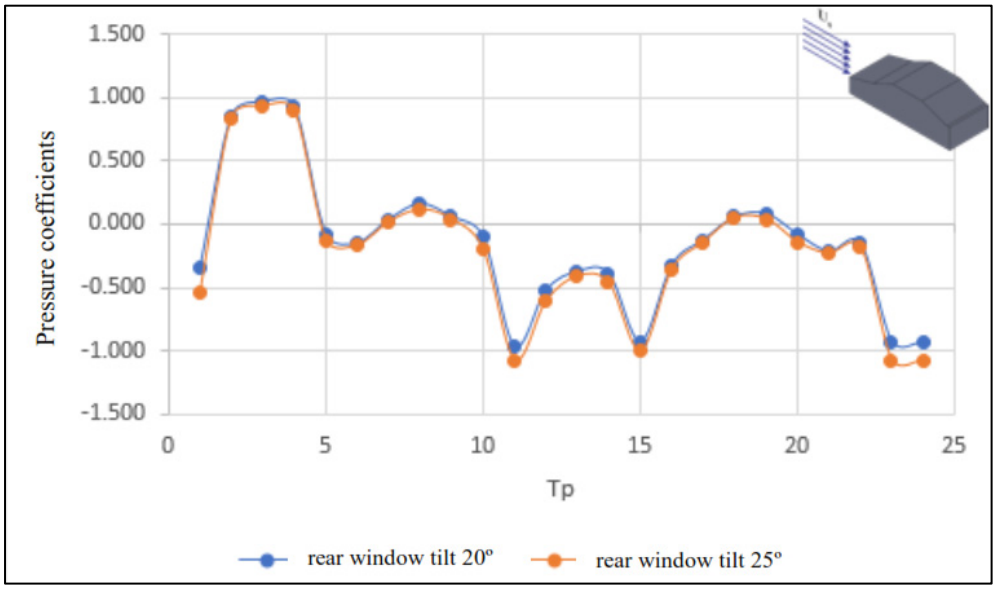

FIGURE 5. Comparison of pressure distribution on 20° and 25° rear window tilts for experimental approach

For the distribution of pressure on the back of the test model with a rear angle of 23º shown in figures 6 and 7. From the graph it can be seen that at the rear angle 23º has a larger distribution when compared to the angle of 25º although the change is not as large as the angle of 20º.

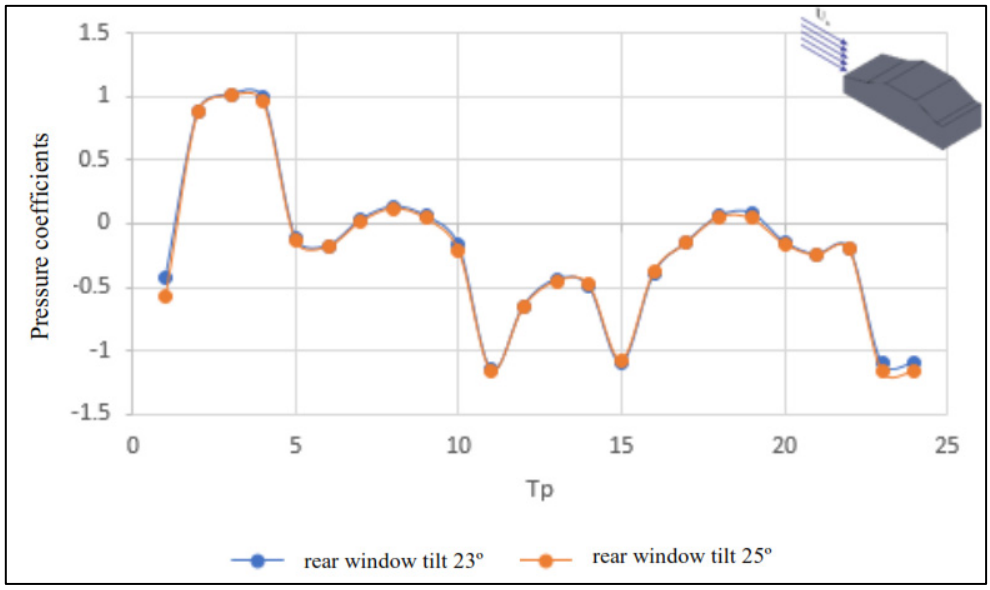

FIGURE 6. Comparison of pressure distribution of 23º and 25º rear window tilts for computational approach

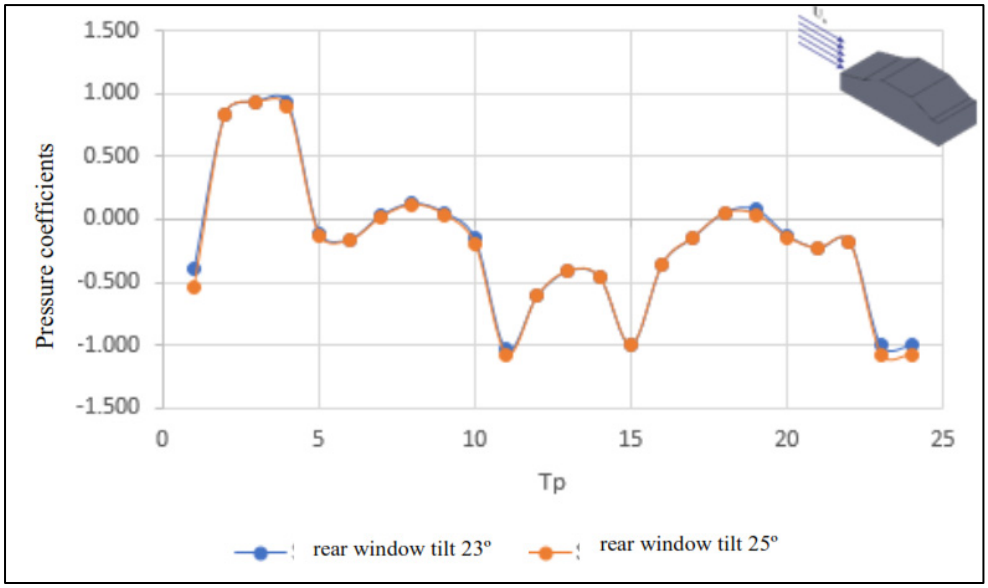

FIGURE 7. Comparison of pressure distribution of 23º and 25º rear window tilts for experimental approach

For the distribution of pressure on the back of the test model with a rear angle of 27o shown in figures 8 and 9. From the graph it can be seen that at the rear angle 27o has a smaller distribution when compared to the angle of 25o. This shows that at that angle it is separation earlier when compared to the angle of 25o so that the pressure on the back area of the model decreases.

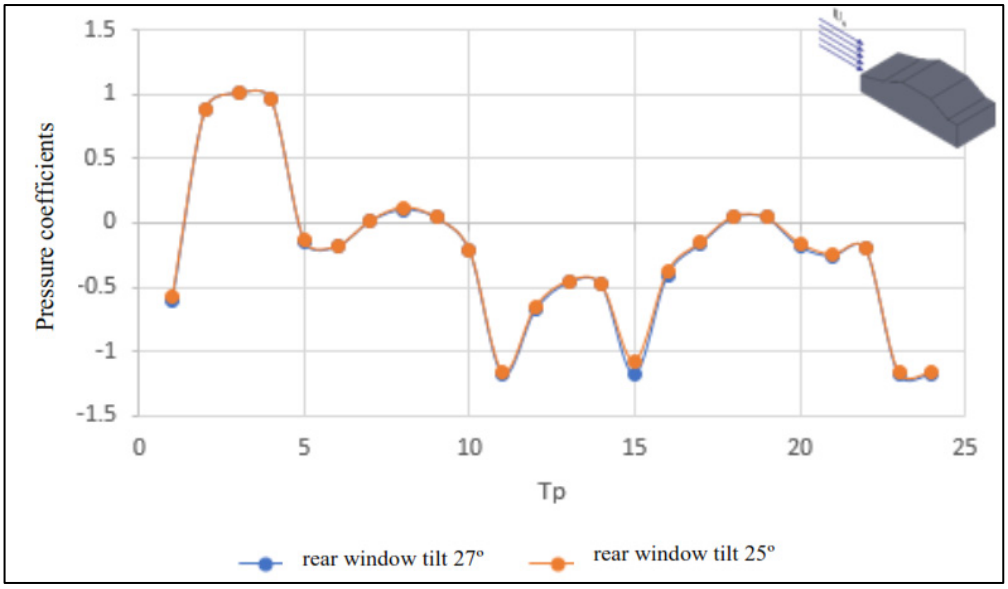

FIGURE 8. Comparison of pressure distribution of 27° and 25° rear window tilts for computational approach

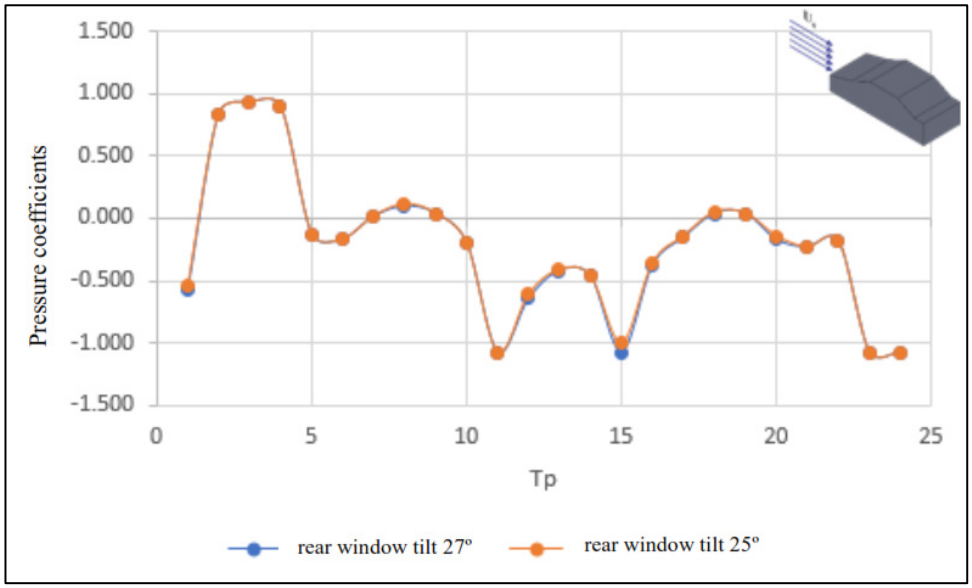

FIGURE 9. Comparison of pressure distribution on 20° and 25° rear window tilts for experimental approach

For the distribution of pressure on the back of the test model with a rear angle of 30° shown in figures 10 and 11. From the graph it can be seen that at the rear window tilt 30° has a smaller distribution when compared to the angle of 25°. at this angle experienced a greater decrease in the pressure coefficient also compared to the angle of 27°.

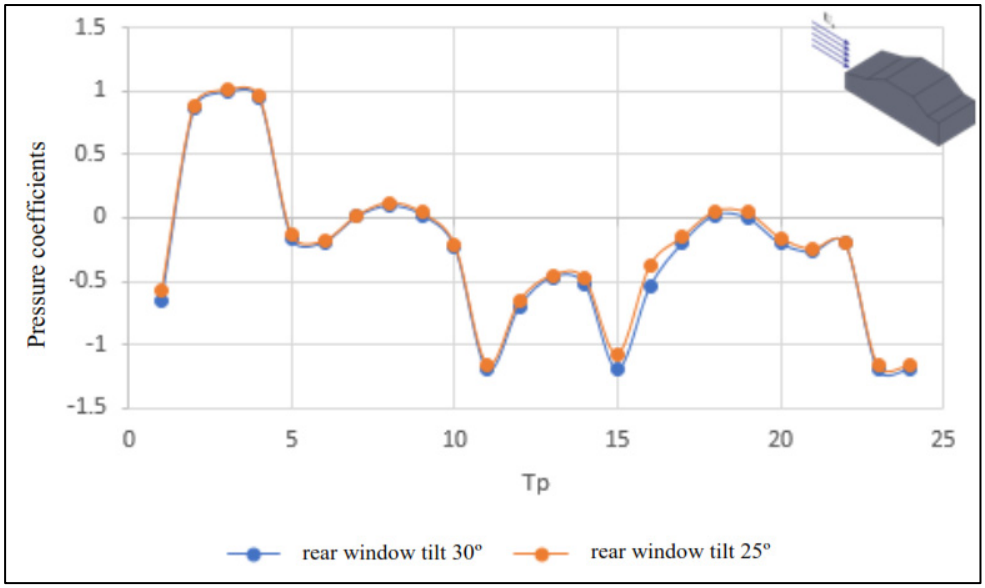

FIGURE 10. Comparison of pressure distribution on 30° and 25° rear window tilts for computational approach

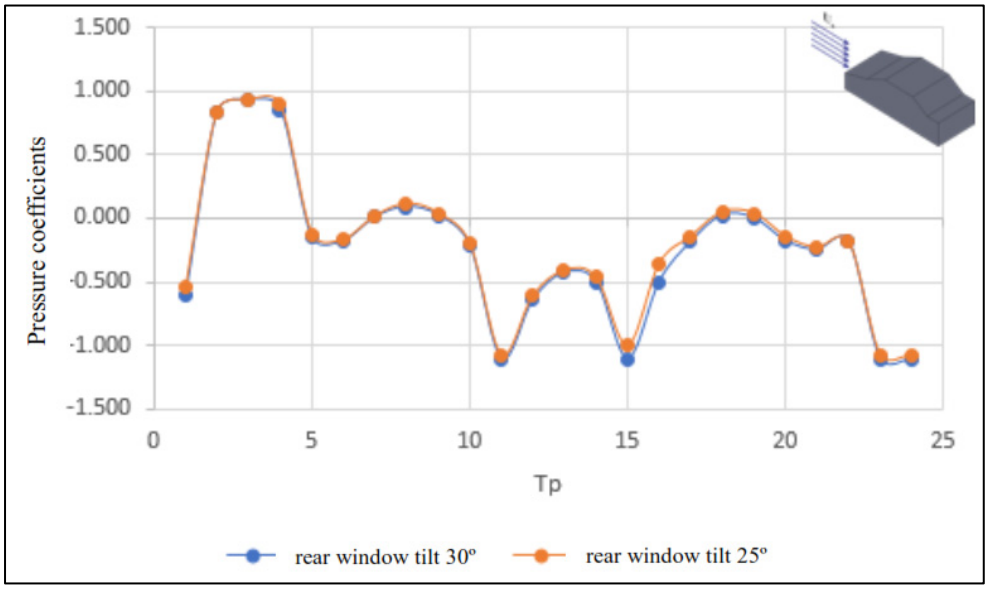

FIGURE 11. Comparison of pressure distribution on 30° and 25° rear window tilts for experimental approach

Drag coefficient

Testing to figure out the value of drag coefficients is done using computational and experimental approaches. The change in angle from the rear window on the test model is intended to reduce the magnitude of aerodynamic drag. To see the effect of the change, a simulation was performed using CD parameters in accordance with the equation in the previous chapter with the density used at 1,225 kg / m3 which is considered constant and the frontal area of the test object of $0.002196^{m2.}$ The data obtained is then displayed in a comparison graph between the drag coefficient (CD) values and the upstream speed. The upstream speed simulated in this study is 19.4 m/s. In this study, the test model with the initial angle of the rear windshield of the sedan car is 25° also simulated with the aim of comparing later with the test model that has a variation in tilt angle. Drag coefficient values can be seen in Figures 12 and 13 as well as Tables 2 and 3.

TABLE 2. Drag coefficient values on the test model with variations in the rear window tilts for computational approach

Upstream velocity	tilt angle				
	25°	20°	23°	27°	30°
11.1	0.731	0.717	0.722	0.738	0.759
13.9	0.712	0.694	0.706	0.717	0.729
16.7	0.691	0.679	0.686	0.700	0.710
19.4	0.678	0.665	0.673	0.685	0.700
22.2	0.668	0.652	0.664	0.671	0.683

TABLE 3. Drag coefficient values on the test model with variations in rear window tilts for experimental approach

Upstream velocity	tilt angle				
	25°	25°	25°	25°	25°
11.1	0.774	0.760	0.773	0.783	0.790
13.9	0.737	0.723	0.735	0.746	0.753
16.7	0.718	0.704	0.716	0.726	0.733
19.4	0.699	0.691	0.697	0.706	0.719
22.2	0.684	0.674	0.684	0.690	0.706

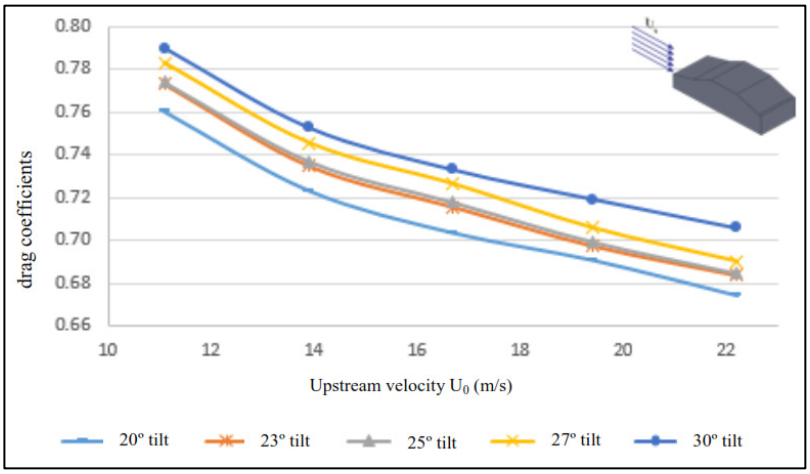

FIGURE 12. Drag coefficient values on the test model with variations in rear window tilts for computational approach

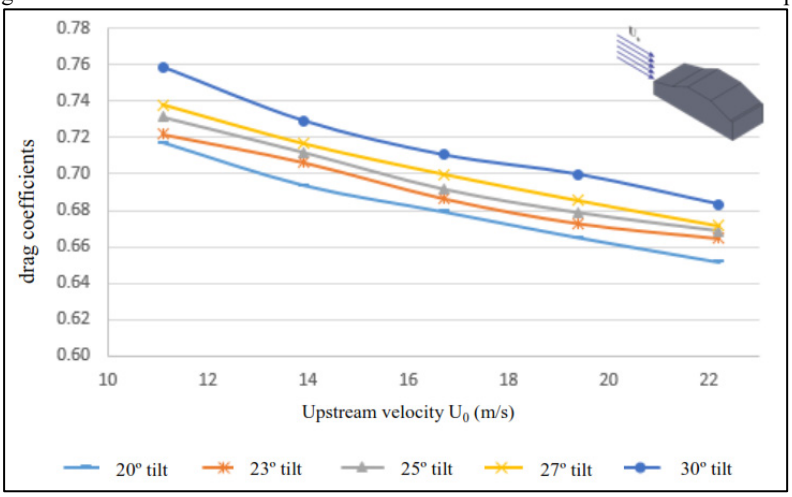

FIGURE 13. Drag coefficient values on the test model with variations in rear window tilts for experimental approach

Based on tables 1 and 2 as well as Figures 12 and 13, a decrease in drag coefficient values at upstream speeds of 19.4 m/s is best at the rear window tilt of 20º. The drag coefficient value at that angle is 0.691 for the computational approach and 0.665 for the experimental approach. This is in line with the results of research conducted by Conan et al for the largest drag value reduction being at the rear window tilt of 20º when compared to the rear window tilt of 25º and the rear window tilt of 30º [11]

CONCLUSION

The change in the angular shape of the rear window has a positive influence on the characteristics of the flow pattern, where there is a delay in flow separation and the largest reduction of the turbulence is at the rear window angle of 20º with an upstream speed of 19.4 m / s. At the pressure coefficient of the rear wall of the vehicle model at the same speed experienced an increase in the value of the highest pressure coefficient, namely at the rear window angle of 20º. And the smallest drag coefficient reduction is at a rear angle of 20º upstream speed of 19.4 m/s, 0.691 for computational approaches and 0.665 for experimental approaches.

ACKNOWLEDGEMENT

The authors would like to express their gratitude to to the Head and Staff of the Fluid Mechanics Laboratory of the Department of Mechanical Engineering, Faculty of Engineering, Hasanuddin University, who have provided facilities for the research.

REFERENCES

1. R. Tarakka, N. Salam, Jalaluddin, W. Rauf, and M. Ihsan, "Aerodynamic drag reduction on the application of suction flow control on vehicle model with varied upstream velocity," *IOP Conf. Ser.: Mater. Sci. Eng.*, vol. 1173, no. 1, p. 012045, Aug. 2021, doi: 10.1088/1757-899X/1173/1/012045.
2. B. Suswanto and N. Finahari, "Studi Pengaruh Model Mobil dan Variasi Kecepatan Angin Terhadap Gaya Drag [Study of the Effect of Car Models and Variations in Wind Speed on Drag Force]," *Widya Teknika*, vol. 21, no. 1, 2013.
3. T. Ragavan, S. Palanikumar, D. Anastraj, and R. Arulalagan, "Aerodynamic Drag Reduction on Race Cars," *Journal of Basic and Applied Engineering Research*, vol. 1, no. 4, pp. 99–103, 2014.
4. W. Hucho and G. Sovran, "Aerodynamics of Road Vehicles," *Annu. Rev. Fluid Mech*, vol. 25, pp. 485–537, 1993.
5. P. Gilliéron, M. Rouméas, and A. Kourta, "Drag reduction by flow separation control on a car after body," *International Journal for Numerical Methods in Fluids*, 2008, doi: 10.1002/fld.1930.
6. B. R. Munson, D. F. Young, and T. H. Okiishi, *Fundamentals of fluid mechanics*, 4th ed. John Wiley & Sons Inc, 2002.
7. R. Tarakka, N. Salam, J. Jalaluddin, and M. Ihsan, "Active flow control by suction on vehicle models with variations on front geometry," *International Review of Mechanical Engineering*, vol. 12, no. 2, pp. 128–134, 2018, doi: 10.15866/ireme.v12i2.13876.
8. Y. Chew, L. Pan, and T. Lee, "Numerical simulation of the effect of a moving wall on separation of flow past a symmetrical aerofoil," *Proceedings of the Institution of Mechanical Engineers, Part A: Journal of Power and Energy*, vol. 212, no. 1, pp. 69–77, 1998.
9. C. H. Bruneau, E. Creusé, D. Depeyras, P. Gilliéron, and I. Mortazavi, "Coupling active and passive techniques to control the flow past the square back Ahmed body," *Computers and Fluids*, vol. 38, no. 10, p. 1875, 2010, doi: 10.1016/j.compfluid.2010.06.019.
10. W. Rauf, R. Tarakka, Jalaluddin, and M. Ihsan, "Effect of Flow Separation Control with Suction Velocity Variation: Study of Flow Characteristics, Pressure Coefficient, and Drag Coefficient," *Universal Journal of Mechanical Engineering*, vol. 8, no. 3, pp. 142–151, May 2020, doi: 10.13189/ujme.2020.080302.
11. B. Conan, J. Anthoine, and P. Planquart, "Experimental aerodynamic study of a car-type bluff body," *Experiments in fluids*, vol. 50, no. 5, pp. 1273–1284, 2011.